Diagn Interv Radiol 2005; 11:182-188

NEURORADIOLOGY

ORIGINAL ARTICLE

Multislice mapping and quantification of brain perfusion MR imaging data: a comparative study of homemade and commercial software

Umut Arıöz, Kader Karlı Oğuz, Senem Şentürk, Ayşenur Cila

PURPOSE

We developed a homemade computer program for analysis of perfusion weighted MR imaging (PW-MRI) data in order to produce colored multislice rCBV, rCBF, and MTT maps. We then compared those maps with others produced by a commercially available program, obtained from the same PW-MRI data, to determine the feasibility of using our program in clinical practice.

MATERIALS AND METHODS

Studies of 20 patients were performed on a high field MR scanner. Imaging protocol consisted of perfusion study (EPI, TR/TE: 1430/46 msec, 10 mm gap, matrix: 128x128, FOV: 240 cm, NEX: 1). Twenty ml of Gd-DTPA was administered at a rate of 4-5 ml/sec beginning at the 5th acquisition of 50 dynamic series. MATLAB software was used for writing codes of both mathematical equations and the graphical user interface. All images were in DICOM standard. For validation of the results, all maps were compared with another commercially available program, which is widely being used in daily practice, and was installed on the MR scanner. Ability to define the lesion contours and extension, and artifacts at the bone-soft tissue interface were the criteria used for statistical evaluation.

RESULTS

Field definition was equally good in 38% of the patient scans for both software programs; our homemade software was better in 23% of the cases and the commercial software was better in 31%. In 6% of the results, either software program was not sufficient. For the elimination of artifacts, our homemade software was 100% successful in every case.

CONCLUSION

Our homemade program is a user friendly one that gives comparable results with those of a commonly used commercial one. However, this program should be tested with different categories of diseases and a larger patient population and then compared with different commercial software programs to be validated more clearly.

Key words: • *brain mapping* • *perfusion* • *brain* • *magnetic resonance imaging*

From the Departments of Medical Education and Informatics (U.A. ✉ *gumuts@hacettepe.edu.tr*) and Radiology (K.K.O., S.Ş., A.C.), Hacettepe University School of Medicine, Ankara, Turkey.

Received 28 March 2005; revision requested 30 April 2005; revision received 19 June 2005; accepted 28 June 2005.

Perfusion weighted magnetic resonance imaging (PW-MRI) is a recently developed technique that can provide information about the functional status of cerebral tissue with a high spatial resolution of morphology and one which has been studied in various diseases of the brain since 1989 (1-3). Using the signal change that brain tissue experiences over time following administration of extracellular gadolinium-based contrast agents, important hemodynamics such as cerebral blood volume (CBV), cerebral blood flow (CBF), and mean transit time (MTT) can be relatively measured and mapped (4). Several manufacturers have developed special software programs to obtain these maps; however, technical personnel needs and high cost of the products have driven many institutions to create their own programs (5, 6). We aimed to develop a computer program, which could work with an MR scanner in an integrated structure, meet our own needs in a standard fashion, and have an open code with which to make modifications that will be required for special research situations when needed. In fact, a simple program that uses just one slice was already developed by the authors and has been used in our institution (7, 8). Lately, we aimed to improve the program in such a way that multislice mapping would be possible with more functionality for both the graphic user interface and mapping of the parameters.

In this study, we used this homemade program for analysis of PW-MRI data to produce colored rCBV (r: relative), rCBF, and MTT maps, and visually compared them to those obtained with a commercial program from the same PW-MRI data to determine its feasibility in clinical practice.

Materials and methods

Data acquisition

Studies of 20 patients were performed on a high field MR scanner (3T, Allegra, Numaris/4, VA21C Release Software, Siemens, Erlangen, Germany). Imaging protocol consisted of perfusion study [echo planar imaging (EPI), TR/TE: 1430/46 msec, 15 slices with a 5 mm thickness and 10 mm interslice gap, matrix: 128x128, FOV: 240 cm, NEX: 1]. Twenty ml of Gd-DTPA was administered at a rate of 4-5 ml/sec, beginning at the 5th acquisition of 50 dynamic series.

Post-processing mapping of the PW-MRI data

Following data acquisition, three slices from the higher probability region of the lesions were selected for calculation. Then, all the images were saved in JPEG lossy compression with 200% zoom factor format (256x256 matrix) in DICOM (Digital Imaging and Communications in Medicine) standard format. DICOM is used for digital images in the field of health sciences, especially in radiology, and stores whole properties of a study

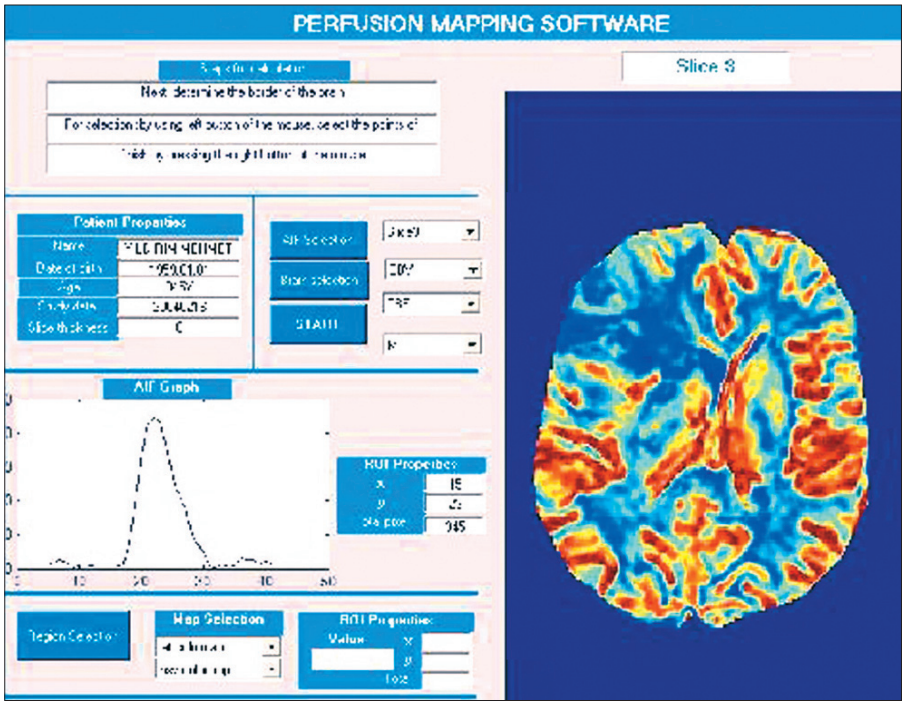

Figure 1. Main window of the homemade software. On the left, patient data list, AIF (arterial input function) graph, and ROI selection and information are displayed. On the right, a cerebral blood flow map (rCBF) of a selected slice is presented.

$$F\{CBF \cdot R(t) \otimes C_a(t)\} = F\{C_t(t)\} = \quad CBF \cdot R(t) = F^{-1}\left\{\frac{F\{C_t(t)\}}{F\{C_a(t)\}}\right\} \quad \text{(Equation 1)}$$

$$CBV \propto \int C_t(t)dt \quad \text{(Equation 2)}$$

$$MTT = \frac{CBV}{CBF} \quad \text{(Equation 3)}$$

$$R(t) : residue\_function$$
$$C_a(t) : arterial\_concentration$$
$$F \;\&\; F^{-1} : discrete\_and\_inverse\_discrete\_fourier\_transform$$
$$C_t(t) : tissue\_concentration$$

Equations 1, 2 and 3.

and patients in 123 different categories. Codes for both image processing and the graphic user interface were written with MATLAB software (Release 6.5, Mathworks Inc., Natick, MA, USA).

One of the important perfusion parameters we studied, CBF, shows the net blood flow through the voxel (2, 9, 10). In calculating CBF, we used model independent (deconvolution)-transform approach (11). In this approach, both arterial input function (AIF), which is selected by the user, and a concentration-time graph of the tissue are automatically calculated pixel by pixel through all images. Following Fourier and inverse Fourier transformations of the graphs, the height of the result shows the CBF value of the pixel (Equation 1, see the box above).

Another important perfusion parameter, CBV, can be determined from the ratio of the area under the tissue and AIF curve. As arterial measurements are not readily quantifiable due to the limited spatial resolution, relative CBV measurements are determined by simply integrating the area under the concentration-time curve (12). According to a recent study (13), numerically integrating the area of the tissue curve over the full time range represents one of the most accurate methods of determining relative CBV. In our study, area under the concentration-time graph of the tissue also gave the CBV measurement (Equation 2, see the box above).

The last important parameter that we focused on, MTT, shows the time that it takes a volume of blood with a certain flow to pass through the voxel (2, 9). From the central volume theorem (14), division of the CBV by CBF value yields the MTT values for each pixel (Equation 3, see the box at left).

All calculations were orderly performed from the first row of the first column to the last row of the last column in the image matrix. For each pixel, an intensity graph was obtained through the whole image series. The resulting image was constructed from the calculations of the graphs that corresponded to the same pixel coordinates with the image series throughout the complete image matrix. At the end of the calculation, the final perfusion parameters' maps were obtained by applying the colormap to the image matrix.

Our program has been developed for easy use, both for physicians and MR technologists. Thus, from the beginning of the procedure, the program directs users with a text message in each step of the calculation until the end. There is a main window that covers the all functions of perfusion mapping. This window contains the four main sections: an instruction part, patient information table, AIF field, and region selection field (Figure 1). A list that shows patient information such as name, age, date of birth, study date, and slice thickness is prepared according to physicians' preferences. With the advantage of open source coding and working with the images in DICOM standard, any information about the patient can be edited, or omitted from the list.

The program was designed in a way that insures each step's instructions are followed by the user, and colored rCBV, rCBF, and MTT maps can be obtained. For starting a calculation of three slices, the user must select one of them as the starting slice. Manual contour drawing is needed to exclude the bone, and this process is applied to the other two slices automatically. For our study, the selection of the slices for each case was based on a predicted location of the lesions, either from previous conventional MR images of the cases, especially of mass lesions, or diffusion-weighted imaging (DWI) in cases of acute stroke, or information given by the physician who performed the clinical examination.

After slice selection, the user must select the AIF for calculations of CBF and MTT. When the AIF selection button is clicked, the computer's mouse becomes the origin point of the coordinate system. By using the left and right buttons of the mouse once, the user marks the point of the diagonal corners of a square or rectangular shape for specifying the region of interest (ROI). In this study, AIF was measured from the middle cerebral artery (MCA) by both our homemade program and a commercial program. The calculation of AIF was done through all perfusion images of the selected area. After the selection of AIF region, the plot of that area is shown on the graph with ROI properties that show the total pixel number and the size of the area in x and y directions. This function can operate in a continuous fashion so that the user can choose the most suitable AIF graph to study.

After selecting the AIF function, the user must mark the borders of the brain parenchyma in order to eliminate the artifacts caused by the brain-bone interface. This can be done by manually drawing the contour of the brain parenchyma, regardless of the shape. Then, that contour is copied onto the same area on the other slices automatically, rather than having to select each slice individually.

After getting the inputs from all three steps, the program is then ready for the calculations. With a click of the 'Start' button, all results of the CBF, CBV, and MTT for each selected slice are prepared in a few minutes and the user can see the percentage of the remaining calculations by following the text field. Within the program, there are different colormap choices for the results. "Jet color map", which ranges from blue to red, and passes through the colors cyan, yellow, and orange, and uses 64 elements to display wider bands of color was preferred in this study to obtain comparable results with the commercial program.

Mathematical values of any desired rectangular or square area, in all color maps, can be obtained by region selection as described above. The same properties of the region in x and y direction can be observed from the ROI properties table as well. For compatibility with other common programs, results can be saved as other image formats (JPEG, TIFF, or DICOM) in the same directory as the patient images.

Table 1. Criteria for data comparison

1	Homemade software is better
2	Commercial software is better
3	Both are good
4	Both are not good

Table 2. Patients in the study

Patient No.	Pathological condition
1	Developmental venous malformation
2	Acute MCA infarction
3	Acute L-MCA infarction
4	Acute R-MCA infarction
5	Moyamoya disease, R-MCA infarction
6	Severe vascular stenosis
7	R- MCA aneurysm
8	Giant R-ICA aneurysm
9	Pre-stenting evaluation-acute infarction
10	Post-stenting evaluation-acute infarction
11	Primitive neuroectodermal tumour
12	Hemangioblastoma
13	Hemangioblastoma
14	Glioblastoma multiforme
15	Medulloblastoma
16	Astrocytoma
17	Meningioma
18	Metastasis
19	Metastasis
20	Metastasis

R: right, L: left, MCA: middle cerebral artery

Evaluation of the maps

PW-MRI data of 20 patients were processed by both our homemade software and a commercially available program, which has been used in daily practice in our institute. Colormaps thus obtained were evaluated visually for each patient by two trained neuroradiologists, separately and then by consensus. Two different properties were rated by the reviewers: 'field-definition' for the identification of abnormalities, especially from the adjacent parenchyma with normal perfusion, and 'artifacts' at the bone and soft tissue interfaces. For each of the two evaluation categories, the evaluators chose from 1 to 4, as explained in Table 1. For enhanced testing of our program's performance, patients with a variety of diseases were studied.

Results

Studied patients included one with a developmental venous anomaly, nine with other vascular conditions such as infarction, Moyamoya disease, vascular stenosis, post-stenting evaluation with acute ischemic lesions, and ten with neoplasms of the brain. Table 2 shows the pathological conditions or reasons for studying the patients. The evaluation results obtained by neuroradiologists are summarized in Table 3. As an example, all the results for all three slices of one patient (patient 17) are shown in Figure 2. Different examples from the results of both the homemade and commercial software can be compared in Figures 3-7.

While field definition was equally good in 38% (n=23) of the patients, using both software programs, our homemade software was superior in 23% (n=14) of the cases and the commercial software was better in 31% (n=19), for all perfusion maps. In 6% (n=4) of the results, both software programs were not sufficient for delineation of abnormalites.

For the second criterion, elimination of artifacts arising at the edges from

Table 3. Summary table for all patients' total CBV, CBF and MTT maps' comparison according to field-definition evaluation

	Comparison of field-definition (see Table 1)			
Parameter (number of patients)	1	2	3	4
CBV (20)	6 (%30)	4 (%20)	10 (%50)	0 (%0)
CBF (20)	3 (%15)	6 (%30)	9 (%45)	2 (%10)
MTT (20)	5 (%25)	9 (%45)	4 (%20)	2 (%10)
TOTAL (60)	14 (%23)	19 (%31)	23 (%38)	4 (%6)

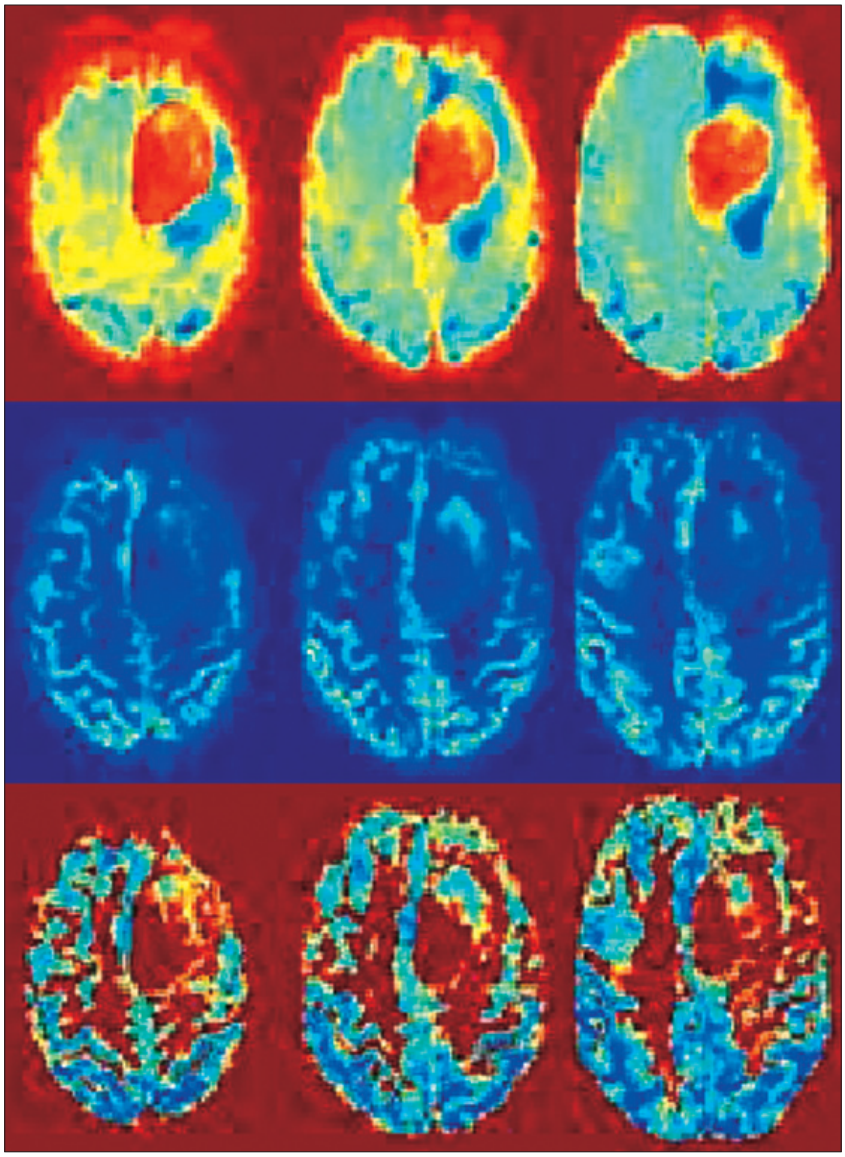

Figure 2. Patient 17. Giant parafalcine meningioma. All three slices for rCBV *(top series)*, rCBF *(middle series)*, and MTT *(bottom series)* maps are seen. The mass has high blood volume and moderate blood flow with a prolonged MTT.

bone-brain interfaces, our homemade software was 100% successful in every case. Naturally, selection of the brain parenchyma at the beginning of the calculations contributed to this result.

Discussion

Perfusion is defined as the volume of blood that passes through a mass of tissue per unit of time. Cerebral perfusion is the steady-state delivery of oxygen and nutrients from blood to cerebral tissue through the capillaries. Since cerebral tissue can get its metabolic needs via perfusion, determination of the perfusion state of the tissue can give an indirect measure of the metabolic activity of that tissue. Physiologically, it must be in the range of 40-60 ml/100g/min for an adult brain (15). Low perfusion might result in cellular ischemia, and high perfusion might be associated with hypervascular lesions such as some tumors (9). Since the first application of PW-MRI on MR, an intense interest has been focused on various diseases that can lead to change in perfusion of the brain parenchyma, in addition to acute stroke, in which tissue at risk is identified (16). During this period, the gold standard for perfusion calculation remains positron emission tomography (PET) (17). PET, however, is available only at a limited number of institutions and requires a prolonged scanning period and repeated arterial blood sampling (18). PW-MRI, due to the wide availability of scanners, and both the short acquisition times and the high resolution that provides enhanced morphological data, has been found to possess superior features in

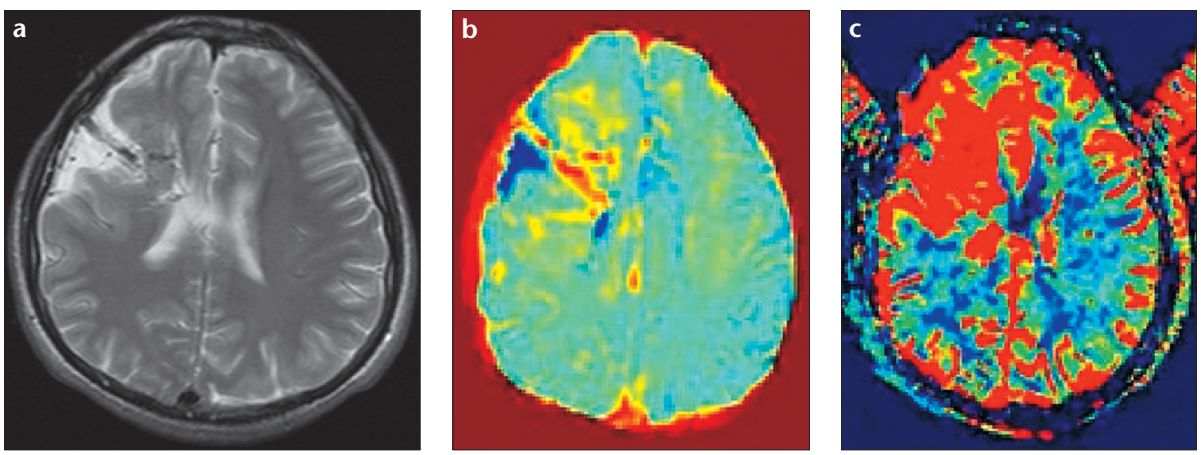

Figure 3. a-c. Patient 1. Relative cerebral blood volume map of a patient with a giant developmental venous anomaly (DVA) associated with cortical dysplasia. Transverse T2-weighted MR image **(a)** shows DVA and cortical dysplasia. rCBV map from homemade software **(b)** and rCBV map from commercial software **(c)** are shown.

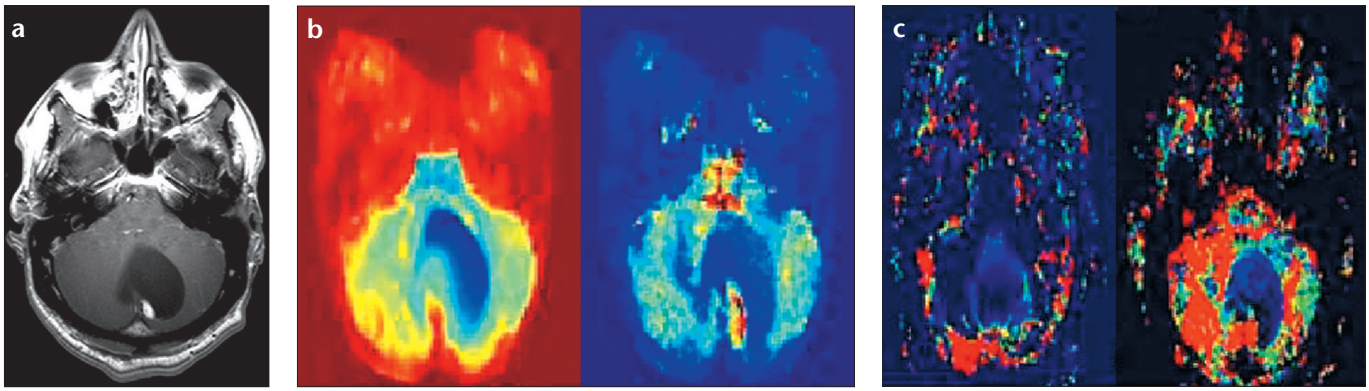

Figure 4. a-c. Patient 12. Transverse post-contrast T1-weighted MR image shows a cystic mass with a mural-enhancing nodule at the medial aspect of cerebellum **(a)**. Corresponding rCBV and rCBF maps of the mass demonstrated with the homemade **(b)** and the commercial **(c)** computer software. The maps from the homemade software show the mural nodule more clearly, and the artifacts at the brain parenchyma and bone interface are reduced in the homemade software. The mass was diagnosed as hemangioblastoma histopathologically.

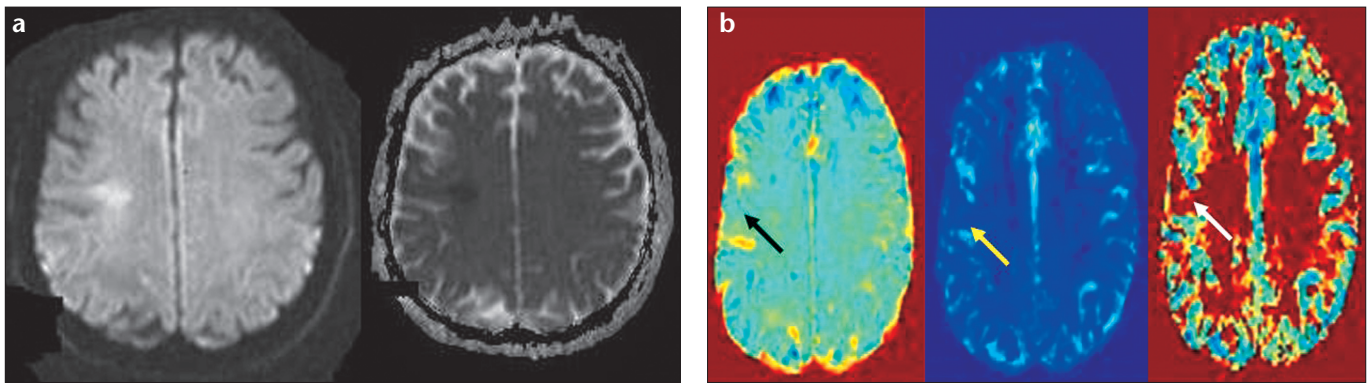

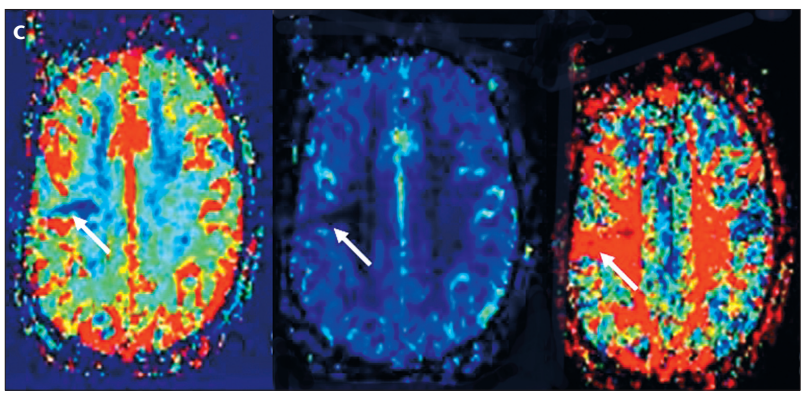

Figure 5. a-c. Patient 10 with a small ischemic area. Trace image of diffusion-weighted MR imaging on the left and apparent diffusion coefficient (ADC) map on the right show the right frontal acute ischemic lesion **(a)**. Top **(b)** rCBV, rCBF, and MTT maps are from our homemade software. Bottom **(c)** maps, in the same order as above, are from the commercial software. Although our program furnished valuable information about the ischemic area, field definition was better in the maps produced with the commercial program. However, with respect to artifacts in the surrounding area, the results of our product were better.

comparison to PET and SPECT in many diseases (19).

There are commercially available computer software programs for qualification and relative quantification of PW-MRI data. However, these products are expensive and rigid, not allowing modifications to be made according to the special interests and needs of physicians. As a result, there has been a great deal of research on developing homemade programs in this field (5, 6, 20). Although our software is simple to operate by both MR technologists and physicians, it still needs to have full integrity with MR scanners. Nevertheless, flexibility to make changes based on special needs, quick calculation of the results, and the mathematical information of ROIs are its important features.

In this study, we chose to assess the criteria separately instead of giving the total percentage values statistically. According to the field definition comparison, successful results of our program covered 61% (23% plus 38%) in total and gave 23% better results. Moreover, according to useful results and from the view of applicable results, our program gave 96% success (except 4% worse results for both software programs) in perfusion parameter mapping). For the second criterion, i.e., artifacts, our program demonstrated superiority and a great advantage over the commercial one. In 100% of the results of the perfusion parameters, our program gave clearer and more suitable results. Considering that radiological work depends directly on image quality, this property has an important impact on diagnosis by radiologists.

In a previous study, we worked on CBV, MTT, and time-to-peak (TTP) (7, 8). The drawbacks of that study was the inability to define AIF, lack of CBF mapping, and working with a single slice.

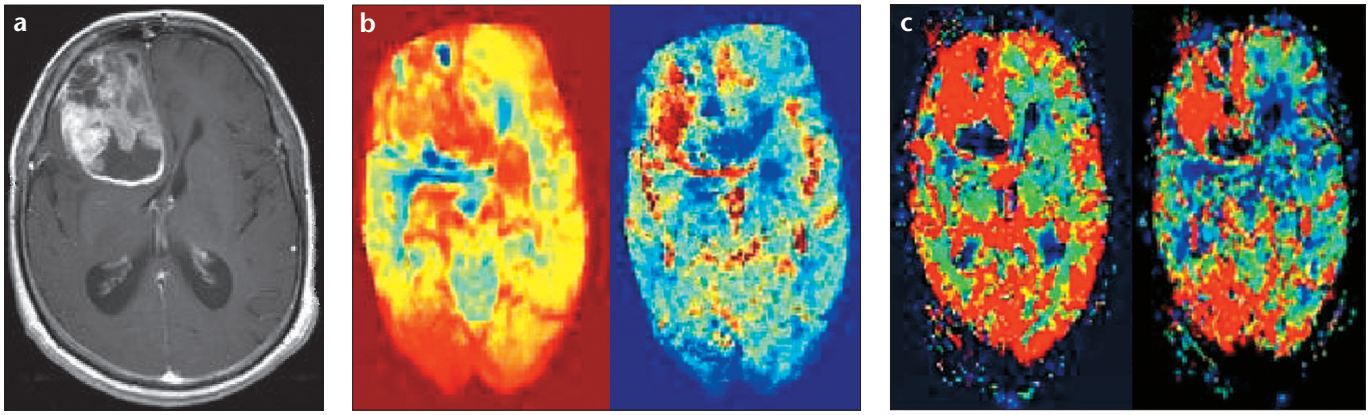

Figure 6. a-c. Patient 14. Transverse post-contrast T1-weighted MR image **(a)** shows a right frontal glioblastoma multiforme. Corresponding rCBV and rCBF maps of the mass obtained from the homemade software **(b)** and the commercial one **(c).** The results are quite comparable, except that there are fewer artifacts in the homemade software.

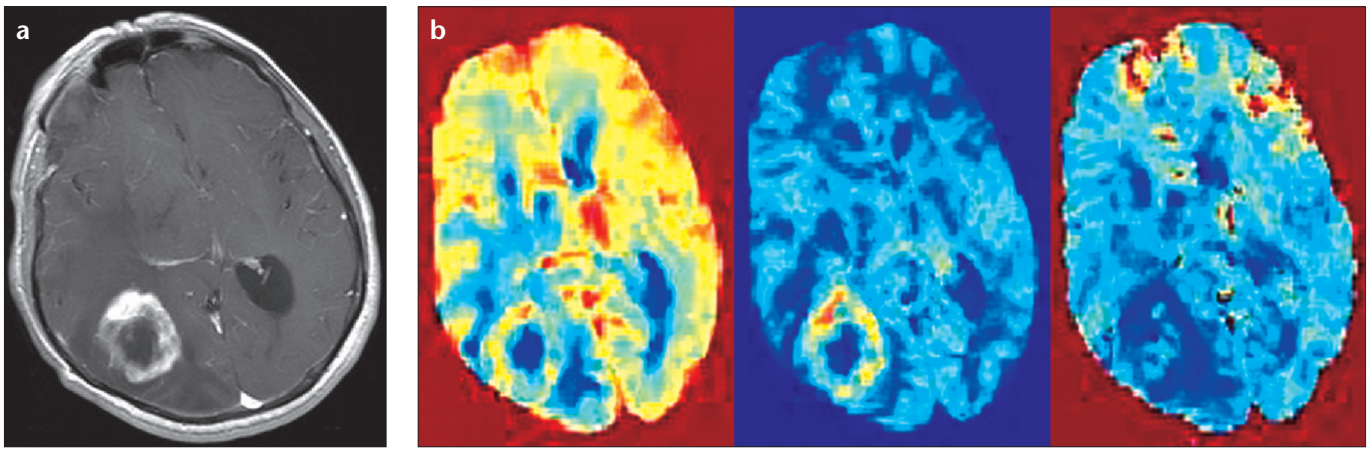

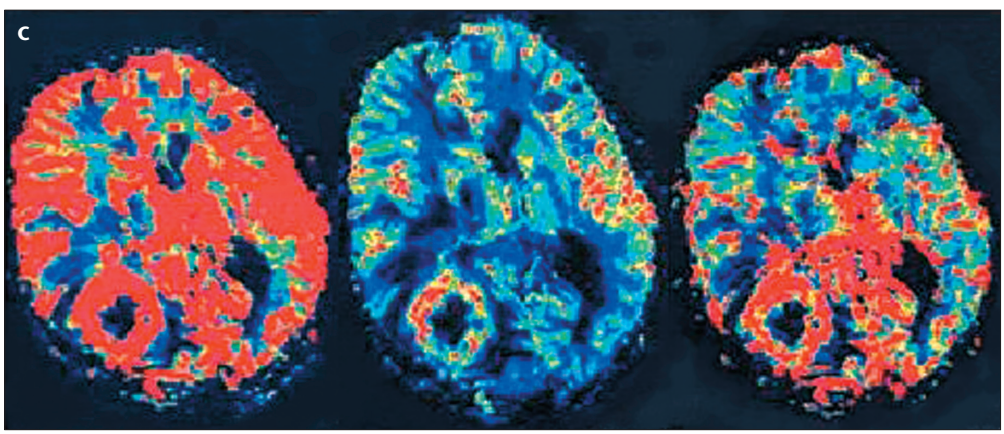

Figure 7. a-c. Patient 18. Transverse post-contrast T1-weighted MR image shows a right parietooccipital metastasis **(a)**. Top row **(b)** demonstrates the homemade rCBV, rCBF, and MTT maps, and bottom row **(c)** shows the commercial software maps of a lung metastasis. The mass shows high rCBF, rCBV, and prolonged MTT at the periphery. The results were quite comparable, except that the field definition in MTT was inferior with the homemade software.

In this current research, we developed a program to overcome the disadvantages encountered in our earlier study. Although we present a three-slice-evaluation report here, our program has the ability to perform whole-brain evaluation with little change, thanks to its open source code.

Another challenge of our study was to implement AIF. The necessity to measure the signal response in the arteries feeding the tissue of interest, so as to differentiate arterial concentrations from tissue concentrations, makes measurement of AIF inevitable. Because a real sampling of the arterial blood is not performed, estimation of the concentration of contrast agent is one of the most challenging issues of PW-MRI studies. AIF signal must have an intrinsic linear relation to the blood gadolinium concentration and should be measured with minimal dispersion and delay compared to the input artery immediately feeding the tissue of interest. High signal-to-noise ratio, intrinsic signal linearity, accurate temporal resolution, spatial resolution, no signal aliasing, same scale as tissue curve, and minimal dispersion and delay are some requirements for determining the AIF. Among the various AIF imaging methods studied, each has advantages and

some disadvantages. The ability to spatially resolve the arterial lumen is improved using larger arteries such as the internal carotid artery (ICA) or the middle cerebral artery (MCA). However, an AIF sampled in a smaller artery would have less dispersion and delay (21).

Another issue with PW-MRI is that it gives the relative amounts of blood volume and blood flow. Examining cerebral tissue without disease at the corresponding location of the opposite hemisphere can give an idea about the relative measures of these parameters. In this study, we did not measure the ratios of these values because we did not aim to explain what changes in perfusion state of the tissue occur in diseases, but only focused on the feasibility of our homemade software.

A graphic easy-to-use interface that precisely instructs the user while the program is running has been developed for our software. This is important because physicians who handle PW-MRI data analysis may be unavailable at the time of immediate evaluation of the data following acquisition. Therefore, anyone who is familiar with a personal computer (PC) can analyze the data.

Decreased susceptibility to subjective threshold settings and standardization of the colors of perfusion maps with already established specific colormaps are other advantages of our program for PW-MRI data analysis. As explained previously in the Methods section, users are directed step by step by text messages throughout the post-processing procedure. This provides for less training time and quick adaptation of the users to the program.

In this study, evaluation of the artifacts at the brain parenchyma and bone interface revealed that the homemade software greatly eliminated much of the artifacts and resulted in clearer images in all cases. Our program's ability to manually define the brain contours has exploited this property.

The main limitation of our software is that it still needs to be completely integrated with the MR scanner. The need to transfer MR images to another computer medium relatively limits its use and increases the time between the data acquisition and the resultant maps. However, once transferred to a PC next to the scanner or a remote location, the total time for analysis of three slices is approximately three minutes, which is no longer than needed by the commercial software.

In conclusion, our homemade program is a user friendly one that yields comparable results with those of a commonly used commercial one. We believe our program should be tested with different categories of diseases on a larger patient population. Those results should then be compared to the results obtained with other commercial software programs to validate our program more clearly.

References

1. Calamante F, Thomas DL, Pell GS, Wiersma J, Turner R. Measuring cerebral blood flow using magnetic resonance imaging techniques. J Cereb Blood Flow Metab 1999; 19:701-735.
2. Barbier EL, Lamalle L, Decorps M. Methodology of brain perfusion imaging. J Magn Reson Imaging 2001; 13: 496-500.
3. Edelman RR, Siewert B, Darby DG, Thangaraj V, Nobre AC, Mesulam MM. Qualitative mapping of cerebral blood-flow and functional localization with echo-planar MR imaging and signal targeting with alternating radio-frequency. Radiology 1994; 192:513-520.
4. Restrepo L, Wityk RJ, Grega MA, et al. Diffusion and perfusion-weighted magnetic resonance imaging of the brain before and after coronary artery bypass grafting surgery. Stroke 2002; 33:2909-2915.
5. Tsushima Y, Funabasama S, Sanada S, Aoki J, Endo K. Perfusion changes of hepatic parenchyma due to infectious hepatobiliary disease: demonstration by perfusion CT. Comput Med Imaging Graph 2003; 27:289-291.
6. Yoshiura T, Mihara F, Kuwabara Y, et al. MR relative cerebral blood flow mapping of Alzheimer disease: correlation with Tc-99m HMPAO SPECT. Acad Radiol 2002; 9:1383-1387.
7. Arioz U, Oguz KK, Baysal U, Cila A, Implementation of a home-made software for quantitative evaluation of perfusion MR imaging. Neuroradiology 2003; S45: S48-S49.
8. Arioz U, Oguz KK, Baysal U, Cila A, Implementation of a home-made software for quantitative evaluation of cerebral perfusion parameters' maps from 3T MR system. Workshop on Quantitative Cerebral Perfusion Imaging Using MRI: A Technical Perspective 2004; 185-186, Venice, Italy.
9. Reimer P, Puskas Z, Starck P. How to PW-MRI. Rivista di Neuroradiologia 2003; Supp2, 16:63-66.
10. Siegal T, Rubinstein R, TzukShina T, Gomori JM. Utility of relative CBV mapping derived from perfusion MRI in the routine follow up of brain tumors. J Neurosurg 1997; 86:22-27.
11. Gobbel GT, Fike JR, A deconvolution method for evaluating indicator-dilution curves. Phys Med Biol 1994; 39:1833-1854.
12. Rosen BR, Belliveau JW, Vevea JM, Brady TJ. Perfusion imaging with NMR contrast agents. Magn Reson Med 1990; 14:249-265.
13. Perkiö JP, Aronen HJ, Kangasmaki A, et al. Evaluation of four postprocessing methods for determination of cerebral blood volume and mean transit time by dynamic contrast imaging. Magn Reson Med 2002; 47:973-981.
14. Stewart GN. Researches on the circulation time in organs and on the influences, which affect it. J Physiology 1894; 15:1-89.
15. Bell BA. A history of the study of the cerebral circulation and the measurements of cerebral blood flow. Neurosurgery 1984; 114:238-246.
16. Le Bihan D., Breton E. MR imaging of intravoxel incoherent motions: application to diffusion and perfusion in neurologic disorders. Radiology 1986; 161:401-407.
17. Baron JC, Frackowiak RSJ. Use of PET methods for measurement of cerebral energy metabolism and hemodynamics in cerebrovascular disease. J Cereb Blood Flow Metab 1989; 9:723-742.
18. Frackowiak R. PET Cerebral Blood Flow Investigation of Stroke. San Diego: Academic Press, 1997; 636-640.
19. Siegal T, Rubinstein R, Tzuk-Shina T, Gomori JM. Utility of relative cerebral blood volume mapping derived from perfusion magnetic resonance imaging in the routine follow-up of brain tumors. J Neurosurg 1997; 86:22-27.
20. Hacklander T, Reichenbach JR, Weule J, Mödder U. An efficient and robust PC program to calculate MR based regional cerebral blood volume maps. Comput Med Imaging Graph 1997; 21:51-62.
21. Conturo TE, Akbudak E, Kotys MS, Markham J. Arterial input functions for dynamic susceptibility contrast MRI: requirements and signal options. Workshop on Quantitative Cerebral Perfusion Imaging Using MRI: A Technical Perspective. Venice, Italy, March 2004.